
August, 1998LHC Project Report 233

TUNE OPTIMIZATION FOR MAXIMUM DYNAMIC ACCEPTANCE, II: $Q_x = 65$, $Q_y = 58$.

Richard Talman

AP Group, CERN
CH-1211, Geneva, Switzerland

ABSTRACT

By minimizing the “figure of merit” FOM (defined in part I¹ to be the fractional reduction in dynamic acceptance) in the presence of nonlinear elements in the LHC, optimal lattice parameters can be determined. Emphasis here is placed on determining the optimal integer tunes in the ranges $59 \leq Q_x \leq 66$, $56 \leq Q_y \leq 63$ in the presence of systematic errors, constant or time-dependent. The fractional tunes (always taken to be 0.28 and 0.31) have been intentionally chosen to avoid low order resonances. Other than chromaticity sextupoles (that keep the chromaticities near zero) the only nonlinear field errors treated are systematic sextupole, octupole, and decapole, all both erect and skew, and only in the main bending elements. Unlike the fractional tunes, for which random sextupole effects are dominant (see part I¹) systematic octupoles, either erect or skew, in conjunction with the chromaticity sextupoles, drive the choice of integer tunes. Making assumptions that appear to be reasonable concerning field errors to be expected, the optimal tunes have been found to be $Q_x = 65$, $Q_y = 58$. Since the optimum is partly based on compensation over single arcs the same choice should also be good for systematic-per-arc errors.

1. Introduction and review of part I

This main part of this report is a series of graphs exhibiting the variation of “figure of merit” FOM over the range of integer tunes studied. It is these plots that permit optimal tunes to be chosen. These plots are derived by “phasor constructions” with one phasor coming from each bending magnet in the LHC. A few of these plots are shown in detail, both to display the procedure, and to serve as a basis for discussion of the likely causes of good or bad behavior. Also numerous spectra obtained by FFT analysis of 1024 turn tracking in the LHC[†] are shown. By correlating these three forms of graph it is possible to corroborate the calculations semi-quantitatively and to come to a reasonably self-consistent and comprehensive understanding of the results.

Some of the main formulas from part I¹ will first be repeated, for minor further specialization, for ease of reference, and to repair some minor misprints. The dynamic acceptance ϵ_{da} is related to the mechanical acceptance ϵ_{mech} by

$$\epsilon_{\text{da}} = \frac{\epsilon_{\text{mech}}}{1 + \text{FOM}} , \quad (1.1)$$

which serves to define the “figure of merit” FOM. The loss of acceptance is due to the deviation from ideal betatron motion caused by the nonlinear elements. Optimal parameters minimize FOM and hence maximize ϵ_{da} . For all investigations the horizontal and vertical emittances were both taken to correspond to 10σ oscillations at the nominal emittances $\epsilon_x = \epsilon_y = 0.78 \times 10^{-8}$ m.

Pure betatron motion on turn number t is described by

$$x_t = a_x \cos \mu_x t, \quad y_t = a_y \cos \mu_y t, \quad (1.2)$$

where phases have been suppressed for simplicity. The effect of nonlinearity is to superimpose on this motion all possible sum and difference combinations of the form

$$\cos(\Omega(m_x, m_y)), \quad \text{where} \quad \Omega(m_x, m_y) = m_x \mu_x + m_y \mu_y, \quad (1.3)$$

where m_x is a positive integer and m_y is any integer. The presence of these terms causes “distortion” and introduces the possibility that a particle will wipe out on a beam scraper

[†] “LHC ring1, version 5.0 in MAD9 SEQUENCE format” dated “18/06/97 09.34.17.

that it would miss as far as its pure betatron amplitude is concerned. In part I¹, formulas for the coefficients of all terms of the form (1.3) from all multipoles are given. The figure of merit FOM is a sum of absolute values of terms, each of which is itself a coherent sum of terms coming from different sources.

Since μ_x and μ_y are incommensurate (because their fractional parts have been chosen to avoid low order resonances) each of the terms of (1.3) has a different tune (as measured, for example, by spectrum analysing a beam position pick-up) and because of their different frequencies the different terms are “incoherent”. One therefore combines their effects by summing the absolute values of their coefficients. The point is that, with incommensurate frequencies, there will eventually come a time when all distortion terms pass through a maximum at the same time, and at the most limiting place in the lattice. On the other hand it is possible for different multipoles and/or different resonances to contribute to any one term of (1.3). These contributions are therefore “coherent” and their coefficients must be added, taking account of phases, before taking absolute values. As always with interference, the sum of contributions of the same magnitude, say 1, can range from 0 (destructive interference—which in our application is good) to 2 (constructive interference—which is bad). Keeping track of these different forms of interference is simple, in principle, less so in practice. Much of part I¹ is devoted to this calculation.

In this way the figure of merit FOM acquires a contribution for each of the (m_x, m_y) contributions. One can distinguish between a horizontal figure of merit FOM_x and a vertical one FOM_y but, for the calculations being reported here, they are simply summed. The contribution to FOM_x from multipole n is given by

$$\begin{aligned}
 FOM_x^{(E/S)}(n; a_x, a_y; Q_x, Q_y) = & \sum_{m_y=(E/S), 2}^{m_y \leq n_{\max}} \left| \frac{\Delta x^{(E/S)}(n; 0, m_y; a_x, a_y)}{a_x} \right| + \\
 + \sum_{m_x=1}^{n_{\max}} \sum_{m_y=(E/S), 2}^{m_y \leq n_{\max} - m_x} & \left(1 - \frac{\delta_{m_y}^0}{2} \right) \left(\left| \frac{\Delta x^{(E/S)}(n; m_x, m_y; a_x, a_y)}{a_x} \right| + \left| \frac{\Delta x^{(E/S)}(n; m_x, -m_y; a_x, a_y)}{a_x} \right| \right).
 \end{aligned} \tag{1.4}$$

The FOM’s for erect/skew multipoles are distinguished by the E/S superscript. These figures of merit are functions of amplitudes a_x and a_y which are however held constant at the previously-stated values. They are also functions of the tunes Q_x and Q_y , both fractional and integer parts. This formula and the next have been simplified somewhat compared

to Part I¹. Since it is possible for different multipole orders to contribute coherently to the same nonlinear harmonic it is, in principle, necessary to work with all multipoles simultaneously, adding amplitudes from different orders before taking absolute values; it is not strictly legitimate to work on one multipole at a time. But the indications are that such “interference” between orders is of little importance and in this paper the multipoles are treated separately.[†] For this reason the functions $\text{FOM}_x^{(E/S)}(n; a_x, a_y; Q_x, Q_y)$ and $\Delta x^{(E/S)}(n; m_x, m_y; a_x, a_y)$ have acquired an extra argument n compared to the previous paper.

As explained in part I¹, it is primarily random errors that influence the optimal fractional tunes, and it was shown there that the presently nominal tunes of (63.28, 59.31) are reasonably close to optimal as far as the fractional parts are concerned (in the small range ($\pm 0.02, \pm 0.02$) studied.) Here we are concerned with finding the optimal integer parts. We will find that this optimum is dominated by systematic field errors, primarily erect and skew octupoles, though the (intentionally present and strong) chromaticity correcting sextupoles cannot be ignored.

Explanation of the summation ranges in Eq. (1.4) will not be repeated from the earlier paper. Individual terms have the form $|\frac{\Delta x^{(E/S)}(n; m_x, m_y; a_x, a_y)}{a_x}|$ and are *fractional* distortions of the betatron motion, scaled so as to contribute directly to FOM;

$$\begin{aligned} \frac{\Delta x^{(E/S)}(n'; m_x, m_y; a_x, a_y)}{a_x} &= \frac{\sin \mu_x \mathcal{R}_{\Omega(m_x, m_y), \mu_x}}{2 \cos \Omega(m_x, m_y) - 2 \cos \mu_x} (1 - \frac{1}{2} \delta_{m_x}^0 \delta_{m_y}^0) \times \\ &\sum_{n'_y \leq n'} \sum_{n'_y = (E/S), 2}^{n'_y} \sum_{k'_y = 0}^{n'_y} \sum_{k'_x = 0}^{k'_x \leq (n' - n'_y)/2} n_{\sigma_x}^{(n'_x - 1)} n_{\sigma_y}^{n'_y} \left(\frac{\epsilon_x}{r_{\text{ref}}}\right)^{\frac{n'_x - 1}{2}} \left(\frac{\epsilon_y}{r_{\text{ref}}}\right)^{\frac{n'_y}{2}} \times \\ &(-1)^{\text{int}(\frac{n'_y}{2})} \frac{1}{2^{n'_y - 1}} \binom{n'_y}{n'_y} \binom{n'_y}{k'_y} \binom{n' - n'_y}{k'_x} \delta_{n'_y - 2k'_y - m_y}^0 \delta_{n' - n'_y - 2k'_x - m_x}^0 \times \\ &\left(r_{\text{ref}}^{\frac{n'_x - 1}{2}} \mathcal{P}_x(n_{\sigma_x}, n_{\sigma_y}; n', n'_y; m_x + 1, m_y) + r_{\text{ref}}^{\frac{n'_y - 1}{2}} \mathcal{P}_x(n_{\sigma_x}, n_{\sigma_y}; n', n'_y; m_x - 1, m_y)\right) \end{aligned} \quad (1.5)$$

Factors like $\binom{n'}{n'_y}$ are binomial coefficients. The factors $\mathcal{P}_x(n_{\sigma_x}, n_{\sigma_y}; n', n'_y; l_x, l_y)$ are “phasor factors”. The prescription for calculating them is given in Part I¹. Here we repeat only Fig. 1.1. The caption gives an essentially complete description of the prescription.

[†] This statement is mildly contradicted in FFT plots shown below which exhibit interference between first order octupole and second order sextupole terms. This interference is not correctly accounted for in the approximation of this paper since the FOM contains only first order terms.

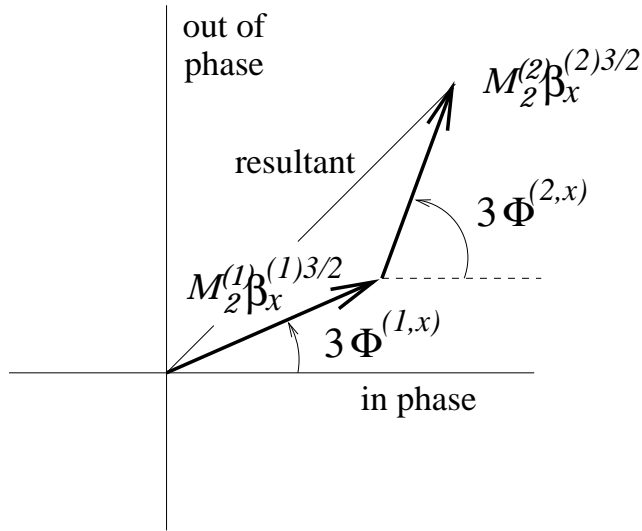


Figure 1.1: Phasor diagram appropriate for superimposing the contributions of two erect sextupoles to the resonance $3Q_x = \text{integer}$ for a deflecting term $l_x = 3$ coming from $n_x = 2$, $k_x = 0$ to obtain phasor \mathcal{P} . For the general resonance the phasor angle is $l_x\Phi^x + l_y\Phi^y$ and the phasor magnitude is $M_n\beta_x^{(1+n_x)/2}\beta_y^{n_y/2}$ for x -response and $M_n\beta_x^{n_x/2}\beta_y^{(1+n_y)/2}$ for y -response.

2. Plots of FOM as a function of Q_x and Q_y

The following several pages contain plots of FOM for all integer tunes in the ranges $59 \leq Q_x \leq 66$, $56 \leq Q_y \leq 63$. For each of these 64 pairs (less pairs with $Q_x = Q_y$ excluded by skew-quadrupole/linear-coupling considerations) the LHC was tuned up with both chromaticities set to +2. This was accomplished using the “arc trombones” described in reference². A brief description is attached to this paper as Appendix A. All lattice tuning and particle tracking was performed using *TEAPOT*.

Plots of FOM are given for purely systematic sextupole, octupole, and decapole, both skew and erect in all cases. In all cases the multipole errors are present only one at a time, and only for main bending elements and have a value 1 “unit” (that is $\times 10^{-4}$) at 17 mm. The format of these plots is indicated by a sample on Fig. 2.2 located at the presently nominal tunes (63, 59). The axes are labelled as real and imaginary parts FOM_r and FOM_i , even though it is only the absolute value of FOM that ultimately matters. A single phasor contribution is shown. Since the coherent sum has been taken already the phasor angle is of no further significance, so only the magnitude is significant and to

indicate this a full circle is drawn through the tip of the phasor. (With different scales on the two axes it looks like an ellipse; it is not shown for the sample.) When there is more than one contribution (as is always the case) the values are accumulated so that the outermost circle describes the sum of all terms, which is to say FOM. In every case the scales are such that FOM=1 coincides with the next grid point. In this way the FOM and tune scales are the same, but it is necessary to add 60 to obtain the integer tunes of any particular FOM plot.

For the assumed field errors the only important contributions to FOM come from the chromaticity sextupoles and from octupole errors, both skew and erect. The superposition of the graphs for these three cases is given in Fig. 2.9. The unambiguous optimum is $Q_x = 65$, $Q_y = 58$. Systematic decapole errors do not affect this optimum. For strength equal to 1 unit, which is already a larger than anticipated systematic decapole error, the contributions to FOM are scarcely visible in Fig. 2.5 and Fig. 2.6. To make these results more visible they are given with five times greater strength in Fig. 2.7 and Fig. 2.8. These figures show that, even if the systematic decapole errors are unexpectedly large, their influence on the choice of optimal tunes will still be weak.

In all these plots the betatron amplitudes were 10σ in both planes. It is conceivable that some otherwise particularly strong resonance is suppressed by this equality. To check against this similar FOM plots with $n_x = 10$, $n_y = 5$ were generated. The tunes $Q_x = 65$, $Q_y = 58$ were optimal for this case as well.

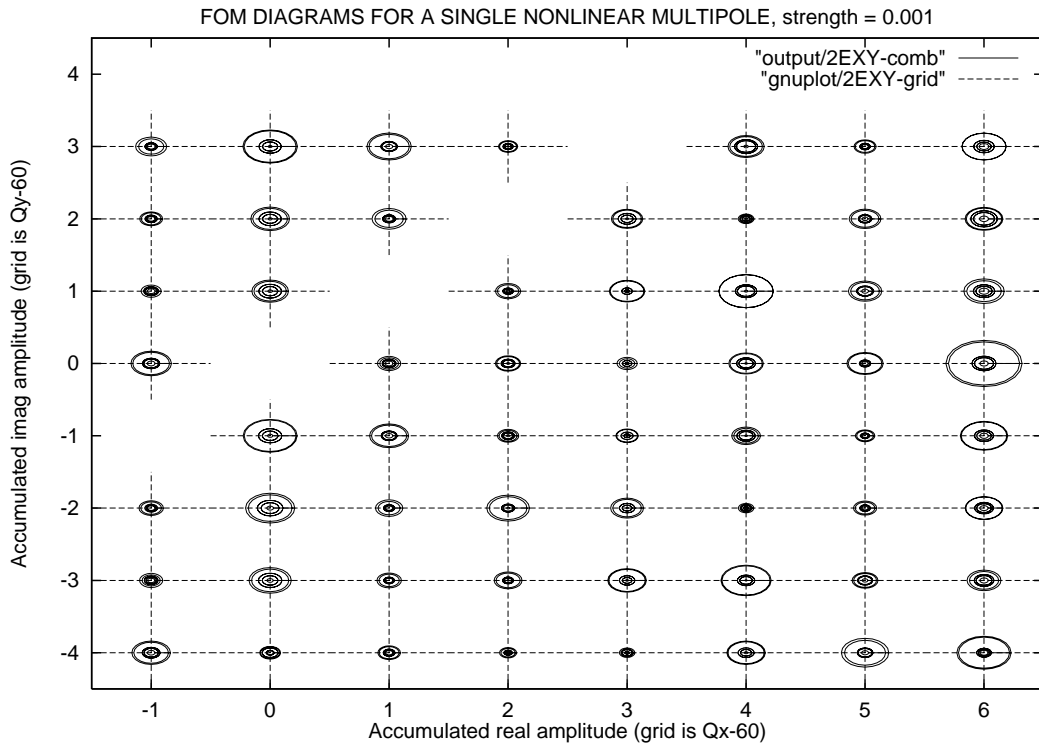


Figure 2.1: FOM values with (erect) chromaticity sextupoles only.

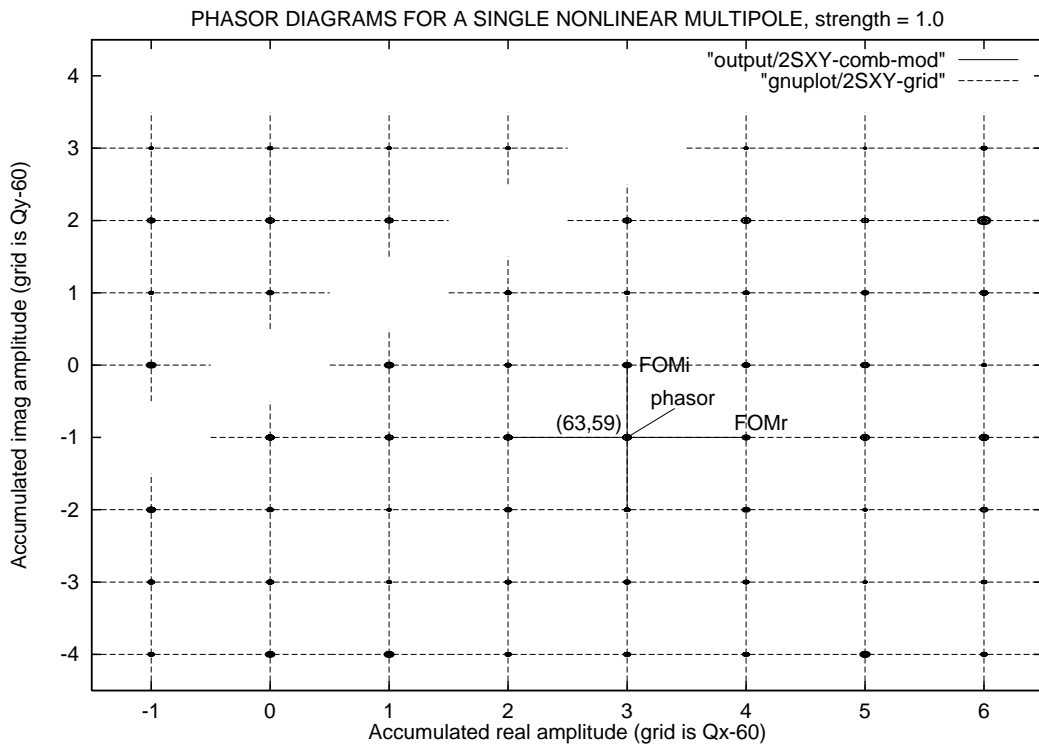


Figure 2.2: FOM values with systematic skew sextupoles errors only. A sample (unreal) phasor is shown in this plot to explain the scales.

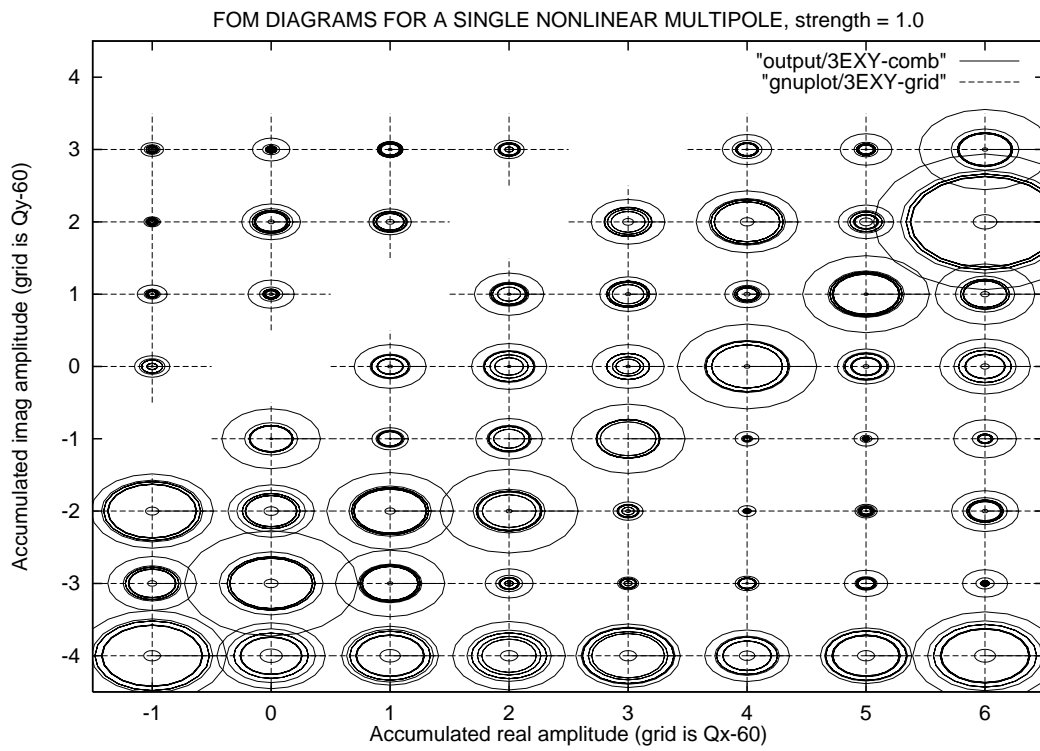


Figure 2.3: FOM values with systematic erect octupole errors only.

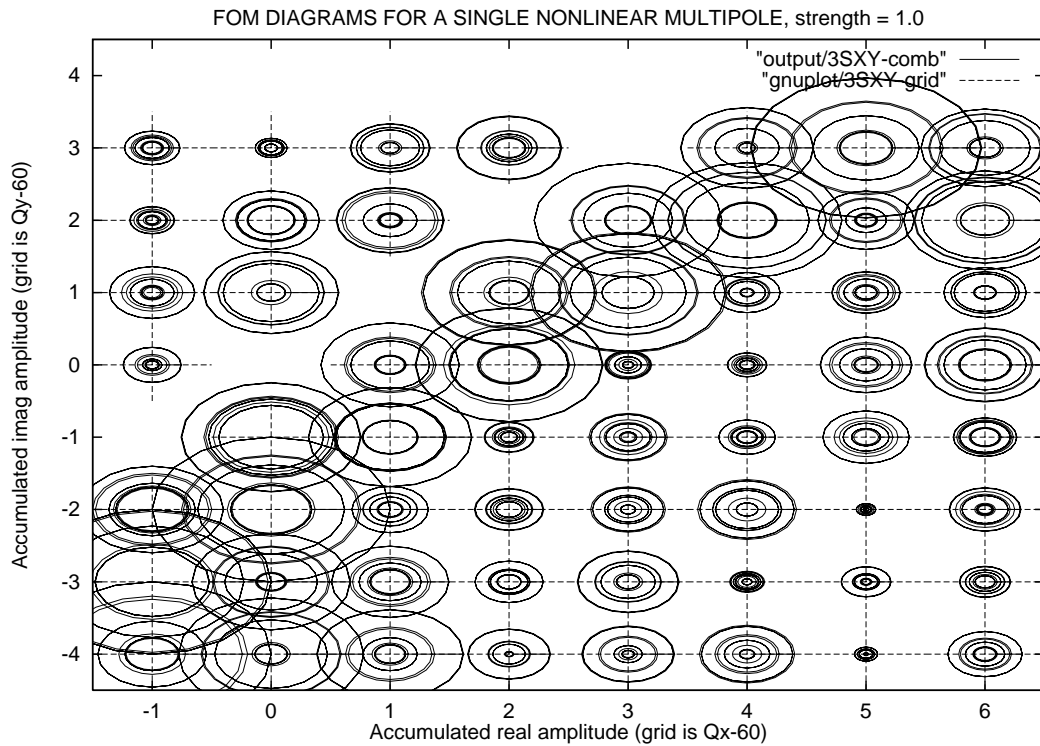


Figure 2.4: FOM values with systematic skew octupoles errors only.

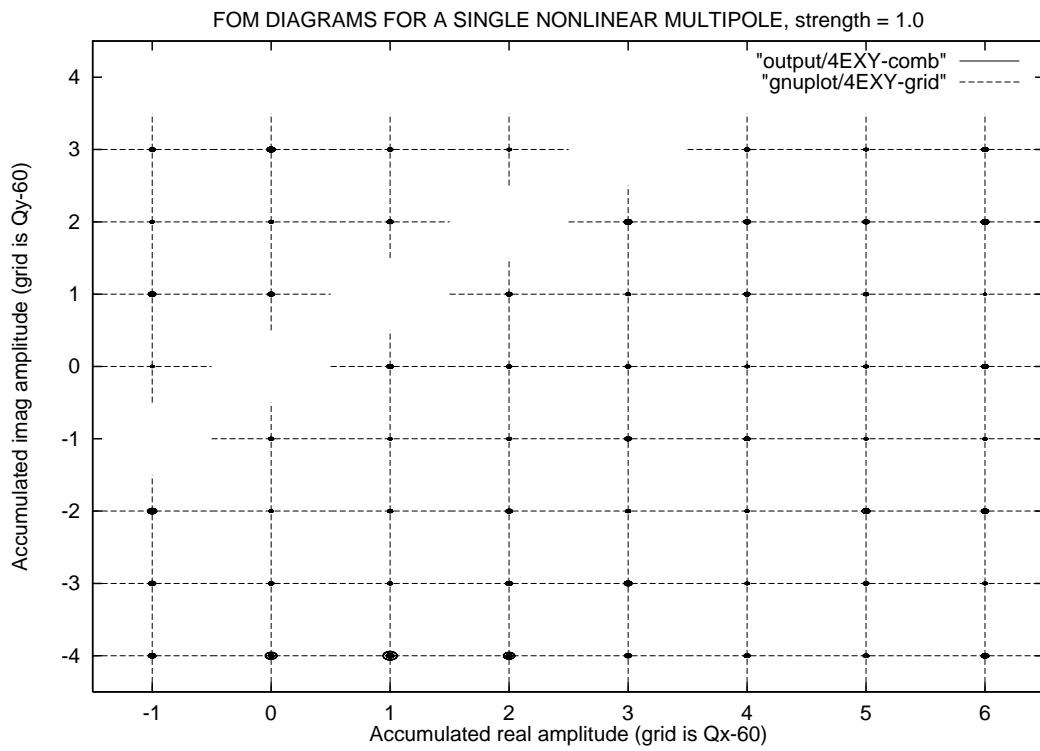


Figure 2.5: FOM values with systematic erect decapoles errors only.

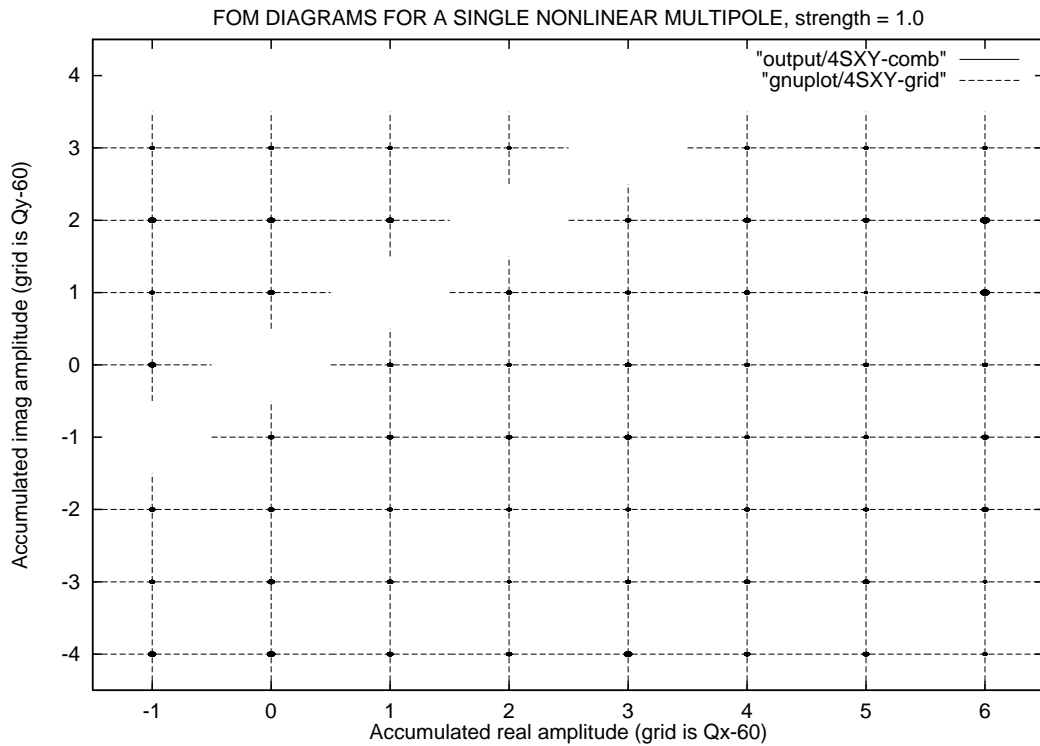


Figure 2.6: FOM values with systematic skew decapoles errors only.

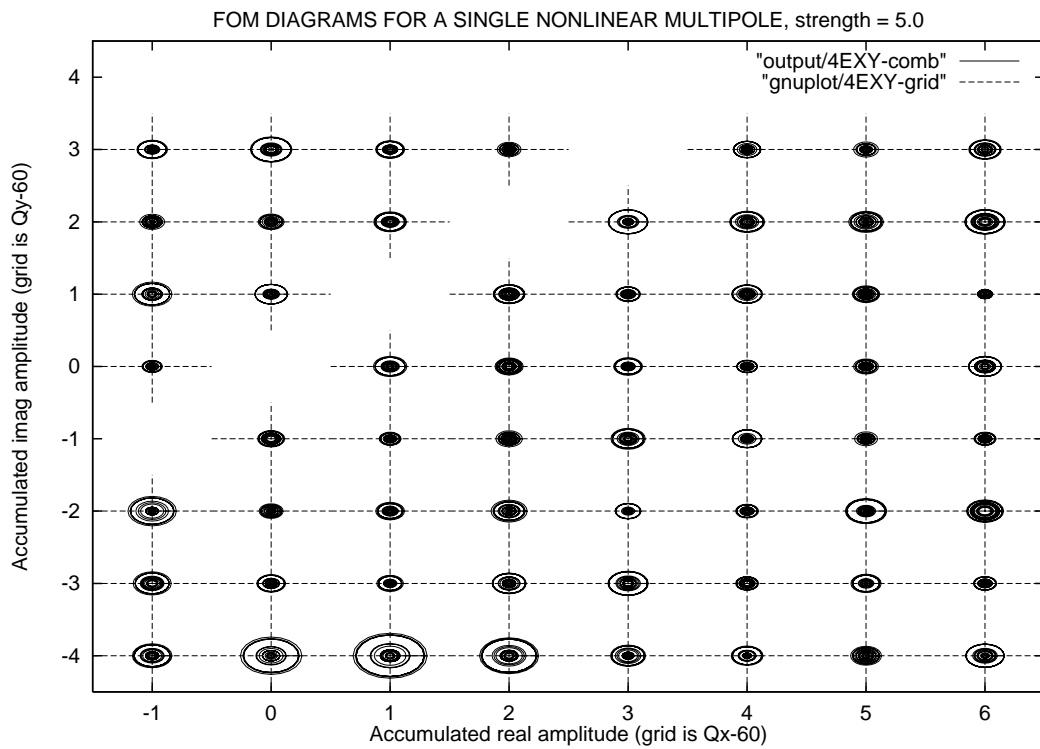


Figure 2.7: FOM values with systematic erect decapoles errors only. To make the curves visible the strength is (relatively) five times too large.

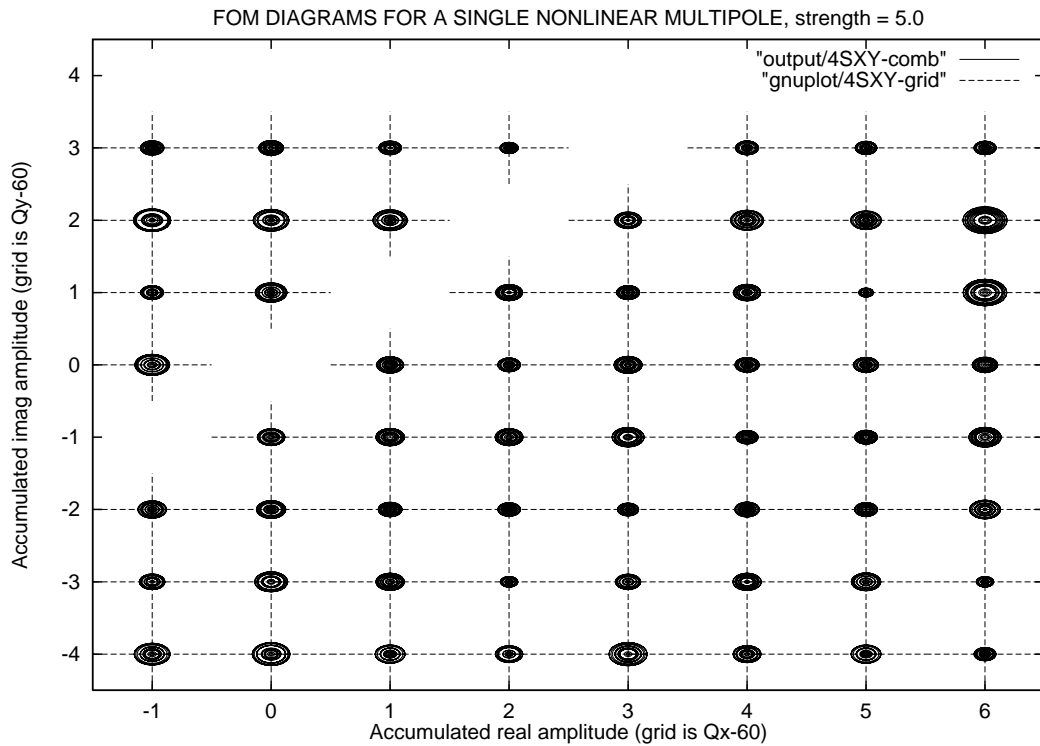


Figure 2.8: FOM values with systematic skew decapoles errors only. To make the curves visible the strength is (relatively) five times too large.

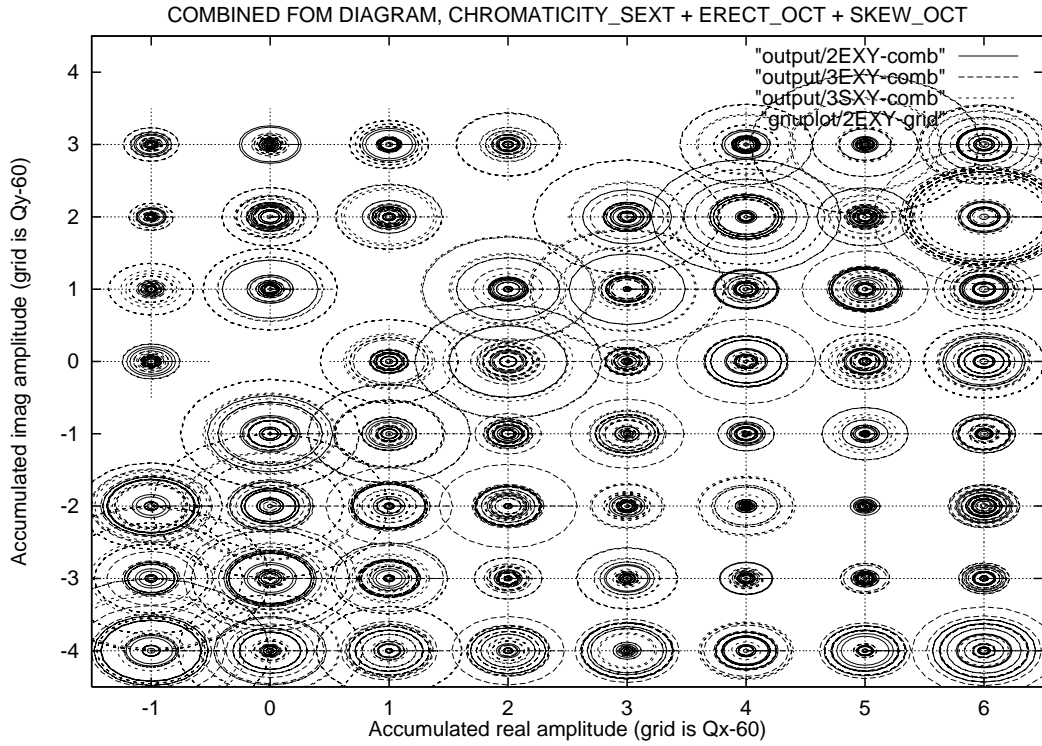


Figure 2.9: FOM values with chromaticity sextupoles plus erect octupole plus skew octupole, all superimposed. The optimal integer tunes are clearly $Q_x = 65$, $Q_y = 58$.

3. Qualitative discussion

Having spent some months working on this problem it embarrasses me to suggest that the essence can be encapsulated in the following two sentences, as expanded upon in the following few paragraphs, and that the major conclusions might therefore have been obtained more simply. In Eq. (1.5) the factor $\Delta x^{(E/S)}(n'; m_x, m_y; a_x, a_y)$ can be large only if both the denominator factor $2 \cos(m_x \mu_x + m_y \mu_y) - 2 \cos \mu_x$ is small and one of the phasor factors such as $\mathcal{P}_x(n_{\sigma_x}, n_{\sigma_y}; n', n'_y; m_x + 1, m_y)$ is large. Laborious as they are to keep track of, the binomial coefficients don't make much difference; they are as often as not equal to 1 and are otherwise small integers that effect the result quantitatively but not qualitatively.

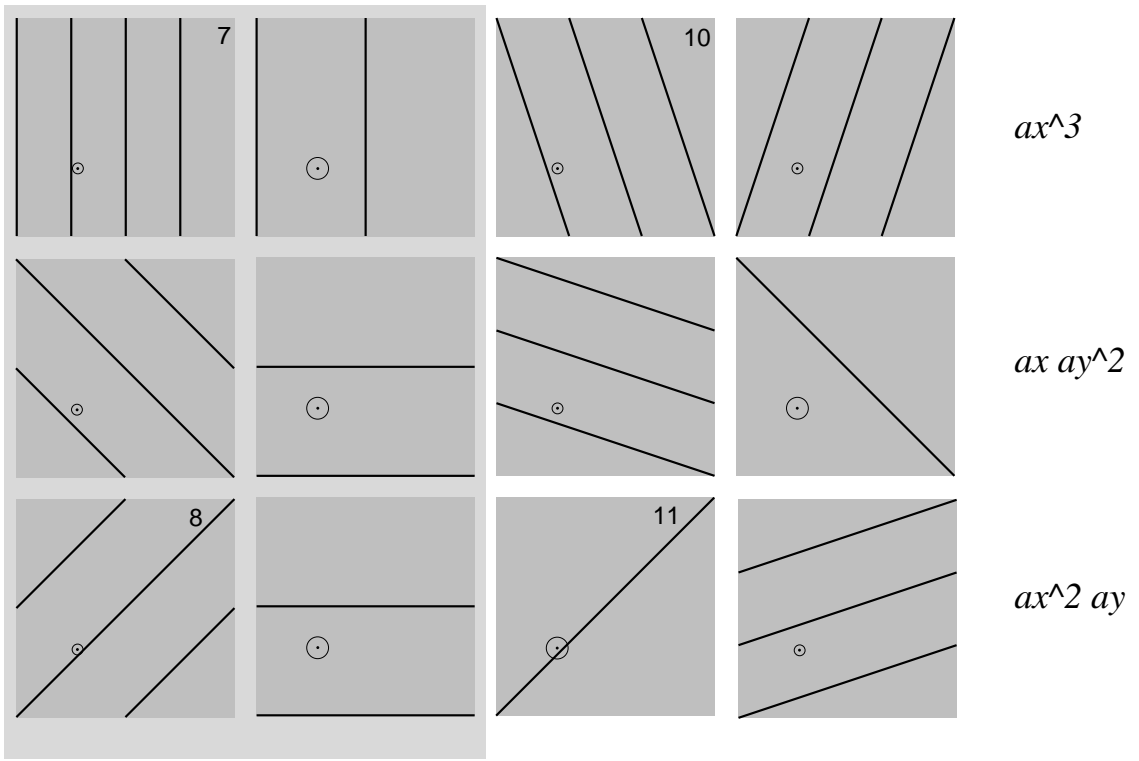


Figure 3.1: A few samples from Part I¹. Resonance lines caused by *octupoles*. Horizontal responses are in the two left columns, vertical responses are in the two right columns. Erect octupoles cause the lines on the left (doubly shaded.) Skew octupoles cause the lines on the right. A possible choice of fractional tunes, $Q_x = 0.28$, $Q_y = 0.31$ is plotted, centered in “circles of influence”. Notations on the left are (n_x, k_x) or (n_y, k_y) or $(n_x, k_x)(n_y, k_y) \pm$ as appropriate. Terms such as $(n_x, k_x) = (3, 1)$ or $(n_x, k_x)(n_y, k_y) \pm = (2, 1)(1, 0) \pm$ that renormalize linear motion have been dropped. A row that would have been labeled $(31)y$ was overlooked in making the figure.

Table 3.1: One line from a table in Part I¹. Potentially important resonances due to *skew* multipoles, based on intersection or near intersection of circles and lines on resonance diagrams, for $Q_x = 0.28, Q_y = 0.31$. $\Delta =$ nearest integer $- 0.28l_x - 0.31l_y$. When l_y is negative the “other” choice is made for k_y . Factors $\binom{n_x}{k_x}$ are not shown since in most cases they are 1.

num.	m-pole	$\binom{n}{n_x} i^{n_y}$	$(\frac{a_x}{2})^{n_x} k_x m_x$	$(\frac{a_y}{2})^{n_y} k_y m_y$	$l_x l_y$	Δ	factor	coeff.
11	oct., $i\Delta y'$	3 -1	$a_x^1/2$ 0 1	$a_y^2/4$ 2 -2	1 -1	0.03	-3/8	2.2362

The denominator factor can, in principle, vanish, and this is the only possibility of “true resonance”. But one chooses the fractional tunes to “stay away from low order resonances”, so the denominator will not vanish in practice. Still, in moving away from one resonance one is inevitably getting close to others, so one has to expect a few of the denominator factors to be small. Note that the denominator factor is not influenced by the choice of integer tunes. As an example some resonance diagrams from Part I¹ are shown in Fig. 3.1 and the relevant parameters for a particular resonance (numbered 11 in both plot and table) are given in Table 3.1. For this point the circle crosses a line in Fig. 3.1—this corresponds to the entry under Δ being smaller than 0.05. The denominator factor is therefore large and the contribution from this term is “big”.

To go from “big” to “gigantic” a term like that just discussed needs to have one of its phasor factors, for example $\mathcal{P}_x(n_{\sigma_x}, n_{\sigma_y}; n', n'_y; m_x + 1, m_y) = \mathcal{P}_x(n_{\sigma_x}, n_{\sigma_y}; n', n'_y; l_x, l_y)$, be large.

The same indices (l_x, l_y) govern both the numerator and the denominator factors, but the combination $l_x\mu_x + l_y\mu_y$ controls coherence turn-by-turn via the denominator, and the combination $l_x\Delta\mu_x + l_y\Delta\mu_y$ governs coherence cell-by-cell via the numerator. Here $\Delta\mu_x$ and $\Delta\mu_y$ are the betatron phase differences between the corresponding elements in adjacent cells. One or the other of the (l_x, l_y) indices differs by ± 1 from the corresponding one of the pair (m_x, m_y) . At the level of trigonometry the source of this numerology is the identity

$$\frac{1}{\cos(m_x\mu_x + m_y\mu_y) - \cos\mu_x} = \frac{1/2}{\sin((m_x + 1)\mu_x + m_y\mu_y) \sin((m_x - 1)\mu_x + m_y\mu_y)}$$

which is the factor describing horizontal response. (The factor governing vertical response is the same except $\cos\mu_x \rightarrow \cos\mu_y$.) For horizontal response the vanishing of one or the other denominator factors is governed by $l_x \equiv m_x \pm 1$ and $l_y \equiv m_y$. For the term mentioned above with number 11 the indices are $l_x = 1, l_y = -1$. This pair will be shown to be “bad” for cell-by-cell coherence in the next section.

The next four figures illustrate phasor constructions for both skew and erect octupoles for both the present nominal tunes (63, 59) and the optimal new tunes (65, 58). In these diagrams there is one phasor contribution from each magnet in the lattice and furthermore

there is a phasor construction for each possible resonance. The individual sums are represented by straight lines. One notices a certain eightfold repetition in these figures and realizes that one can distinguish arc-by-arc contributions to the phasor sum. One then sees that in the (65, 58) case there is approximate cancellation (destructive interference) per arc and an overall favorable compromise per ring. In the (63, 59) case there is constructive interference per arc in both cases and constructive interference also over the whole ring in the erect case. This accounts for the relative superiority of the integer tune combination (65, 58), at least as far as systematic octupole errors are concerned.

The reason octupoles have been discussed is that the FOM figures show them to be dominant. Why is this? The angle between the phasors due to two elements is $l_x \Delta\mu_x + l_y \Delta\mu_y$. For \mathcal{P} to become really large it is necessary for the phasor contributions from successive cells to be approximately parallel. With the integer tunes being approximately equal, the phase advances per cell are also approximately equal. One way for this condition to be met therefore, is for $l_x = -l_y$. In lowest order this condition can only be met for odd (American) multipoles. (See Tables 9.1 and 9.2 of Part I¹.) The lowest (and hence dominant) odd nonlinear multipole is octupole.

Multipoles in adjacent cells can also add constructively if $l_x \mu_x + l_y \mu_y$ is a multiple of 2π . Since phase advance per cells μ_x and μ_y are approximately $\pi/2$ this requires that $l_x + l_y = 4$. This condition can be met for octupoles but not for sextupoles or decapoles. (See Tables 9.1 and 9.2 in Part I¹.)

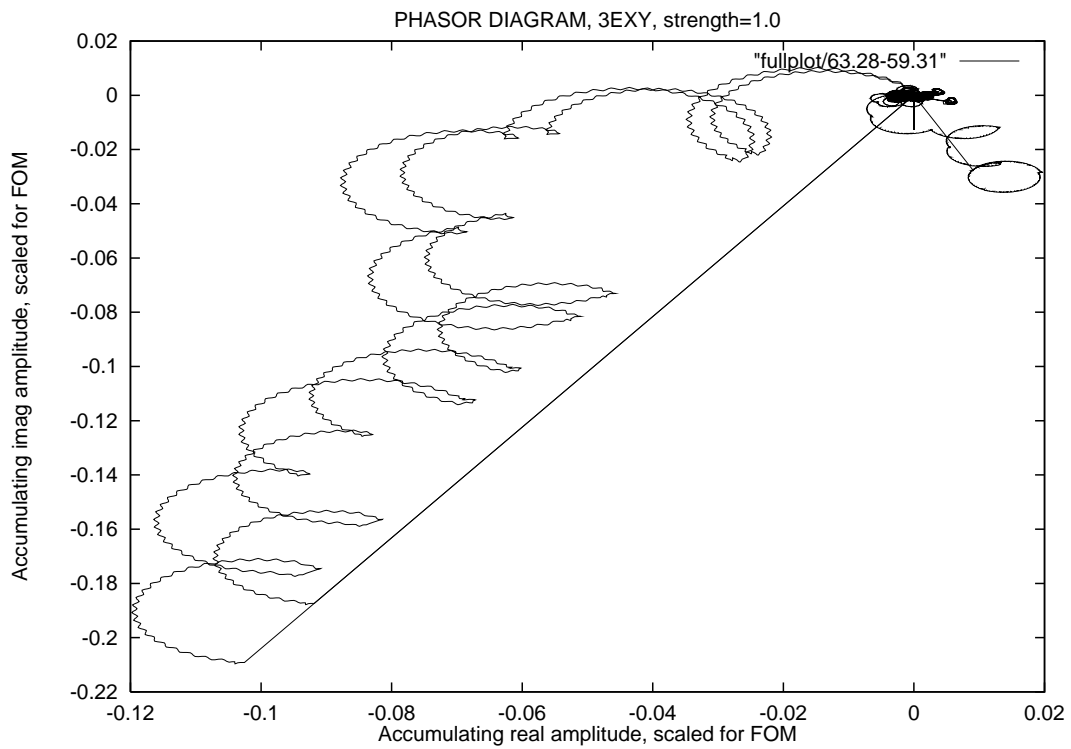


Figure 3.2: Phasor construction for systematic erect octupole errors in the main bend magnets for presently nominal (63,59) integer tunes.

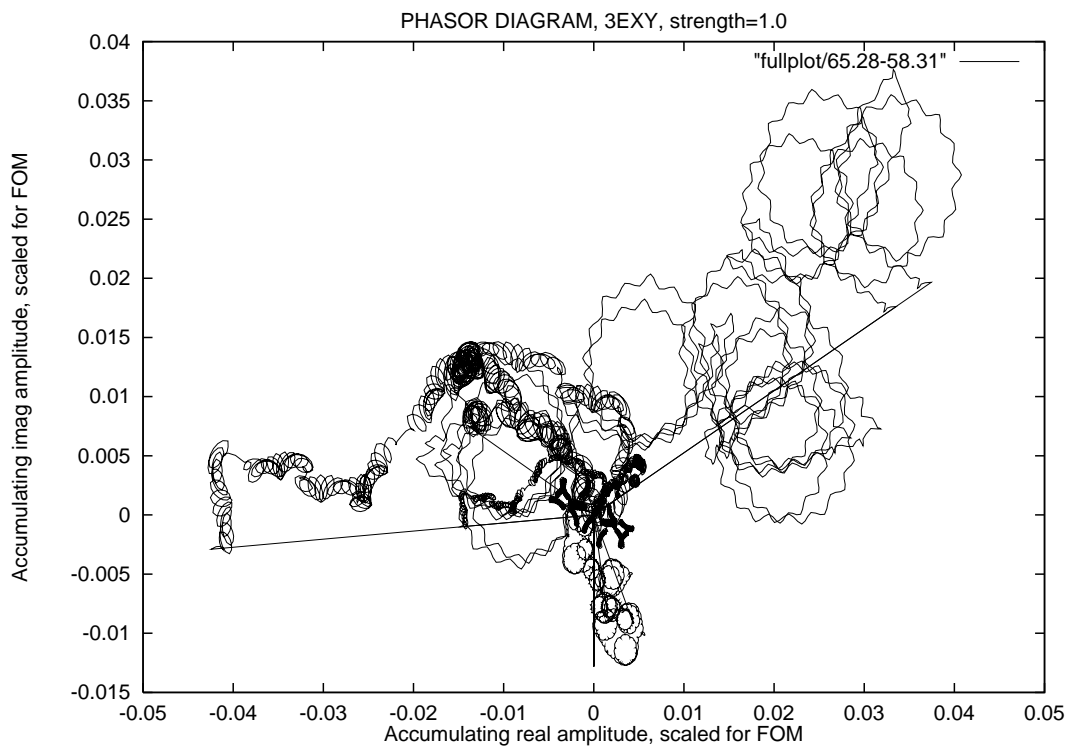


Figure 3.3: Phasor construction for systematic erect octupole errors in the main bend magnets for optimal new (65,58) integer tunes.

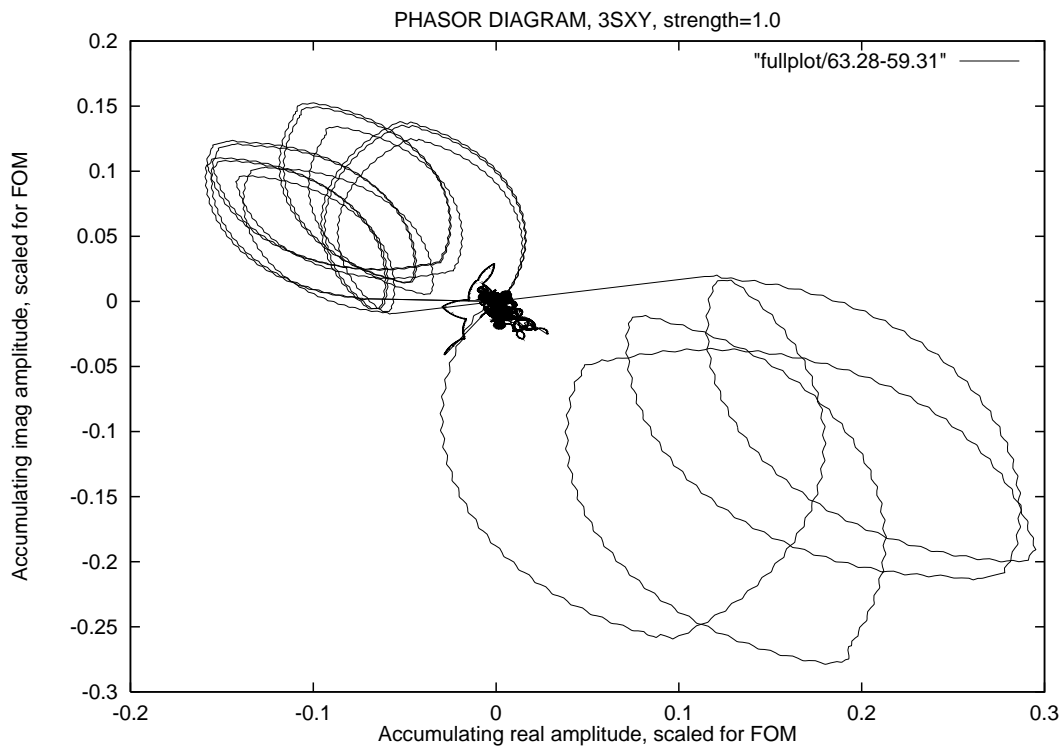


Figure 3.4: Phasor construction for systematic skew octupole errors in the main bend magnets for presently nominal (63,59) integer tunes.

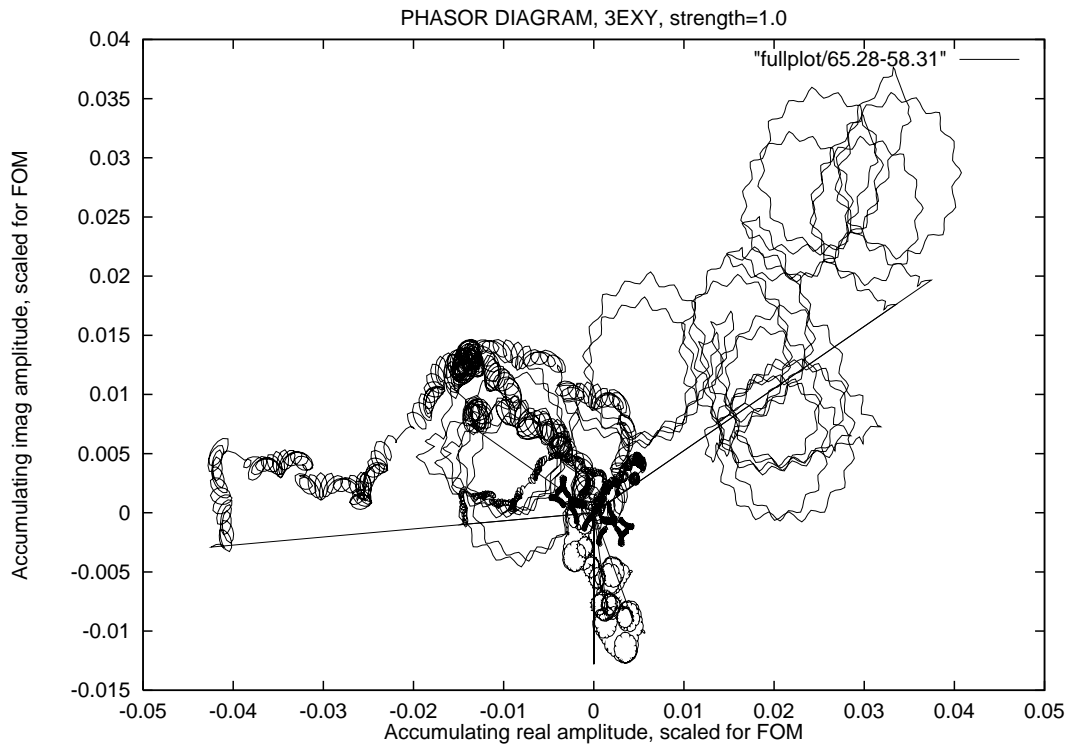


Figure 3.5: Phasor construction for systematic skew octupole errors in the main bend magnets for optimal (65,58) new tunes.

4. Comments on tune spectra obtained from tracking

The next six pages contain tune spectra obtained by post-processing turn-by-turn data for (10σ in both planes) particles in the LHC tracked for 1024 turns using *TEAPOT*. The same cases of assumed field errors are shown, except that the systematic errors are in every case 0.1, ten times less than for the FOM calculations. The purpose in reducing these strengths was to reduce the strength of response due to more than one nonlinear element and hence make the spectra more easily interpretable—one anticipates, after all, that 10σ is a rather large amplitude at which chaotic motion is already likely for realistic field errors. Of course the chromaticity sextupoles were run at the full strength required to produce the correct chromaticities.

In every case the upper plot is obtained by FFT spectral analysis of horizontal positions and the lower plots are the same but for vertical motion. The center of the largest horizontal (respectively vertical) peak is accepted as Q_x (respectively Q_y). The entire spectrum is then normalized to make this line have unit amplitude or, since it is the (natural) logarithm that is plotted, to make this peak coincide with the upper edge of the graph where the logarithm is zero. All the dashed vertical lines in these figures are then dead-reckoned from these tune based on the combinations $m_x Q_x + m_y Q_y$ for combinations of $|m_x|$ and $|m_y|$ adding to 3 or less (except for the decapole plots, in which case $|m_x| + |m_y| \leq 4$). Tunes lying outside the range $0 \leq Q \leq 0.5$ are “aliased” into this range. In every case (except one that will be discussed further below) there is agreement between theory and tracking as to what lines should be observed. This corroborates the overall approach at least as far as establishing that the terms contributing to FOM are the same terms that are observed in the spectra.

A factor that complicates the spectra is that the chromaticity sextupoles, being at full strength as just stated, were strong enough to cause second order lines. In Fig. 4.1 and Fig. 4.2 nonlinear spectral lines can be due only to these sextupoles and the lowest order response satisfies $|m_x| + |m_y| = 2$. The strongest horizontal lines $(m_x, m_y) = (2, 0)$ and $(0, 2)$ and vertical lines $(m_x, m_y) = (1, 1)$ and $(1, -1)$ satisfy this condition, but there are also clear lines for $(m_x, m_y) = (1, \pm 2)$ and $(2, \pm 1)$. In lowest order these lines would come only from octupoles but here they are evidence of second order sextupole terms. Since

the chromaticity sextupoles are always turned on, all the lines in these two plots have to be regarded as “background” as far as diagnosing the effects of other multipoles. An unfortunate consequence of this is that the lines from sextupoles for which $|m_x| + |m_y| = 3$ complicate the interpretation of octupole lines for which $|m_x| + |m_y| = 3$ in lowest order. These lines “interfere”, sometimes constructively, sometimes destructively, which makes it impossible to compare their strengths with calculation with any accuracy.

Apart from this limitation, in principle the strengths of the spectral lines should be accurately predicted by formula (1.5). In practice, there are other factors that restrict the accuracy of these comparisons. With the spectral lines typically having widths of one or two bins there is a “binning problem”. Even the central tune lines may lie all in one bin or be split into two adjacent bins so there can be close to a factor of two uncertainty just based on the normalization of the spectra. This effect is most pronounced in a comparison between Fig. 4.2 and Fig. 4.6. When these spectra are overlaid they appear quite different, but the effect is primarily because the “floor” of the latter spectrum is artificially raised by the binning effect. For the comparisons to be mentioned shortly the strengths of all lines were taken to be the sum of three adjacent bins.

Another effect that limits accuracy is that weak lines can interfere with the “floor” signal in ways that are specific to the FFT process. This can cause lines to be “bipolar” or even negative, making their strengths ambiguous.

For purposes of comparing calculation and tracking, the “cleanest” lines are those due to skew octupoles since these lines are absent from the pure chromaticity sextupole spectra. The comparisons are shown in Table 4.1. The accuracies are 20% or better.

The spectra due to systematic decapoles are Fig. 4.9 and Fig. 4.10. These are “busier” because more lines are possible in lowest order. Again there is good agreement between expected and observed lines. There is however a line at $Q_x = 0.22$ that is not expected to lowest order. This line presumably comes from conspiracy with the chromaticity. Being a relatively strong signal (e^{-6} relative to the fundamental line) a line like this has to be viewed as evidence for insipient chaos. Had this line coincided, or approximately coincided with one of the pre-existing lines (of which there are about 10 in this plot) one could say the Chirikov condition (or a plausible variant thereof) for onset of chaos had been met.

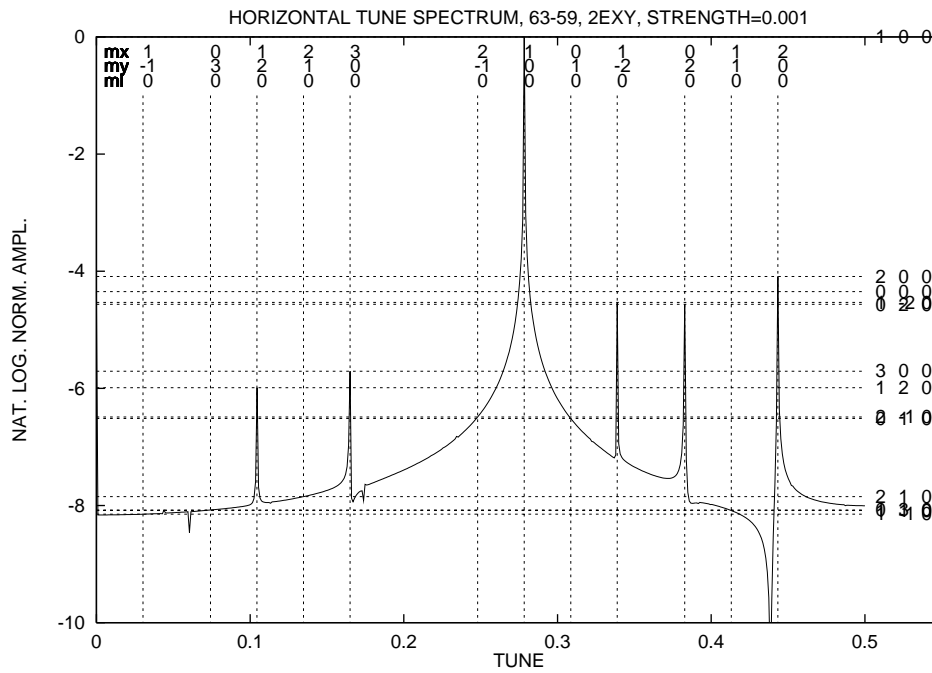


Figure 4.1: Spectral analysis of horizontal motion with chromaticity sextupoles only and presently nominal tunes (63.28,59.31).

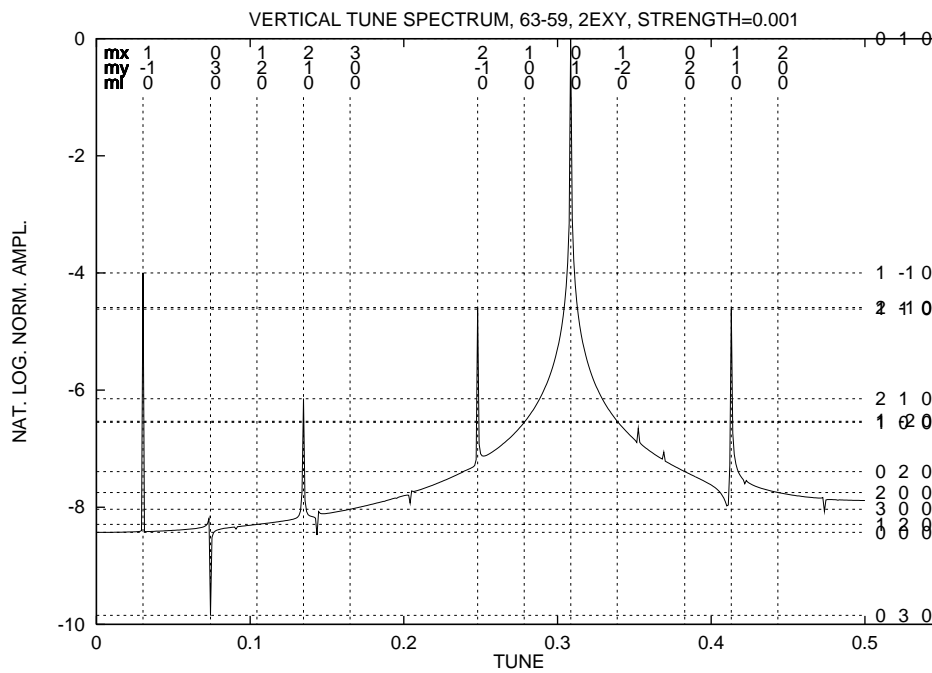


Figure 4.2: Spectral analysis of vertical motion with chromaticity sextupoles only and presently nominal tunes (63.28,59.31).

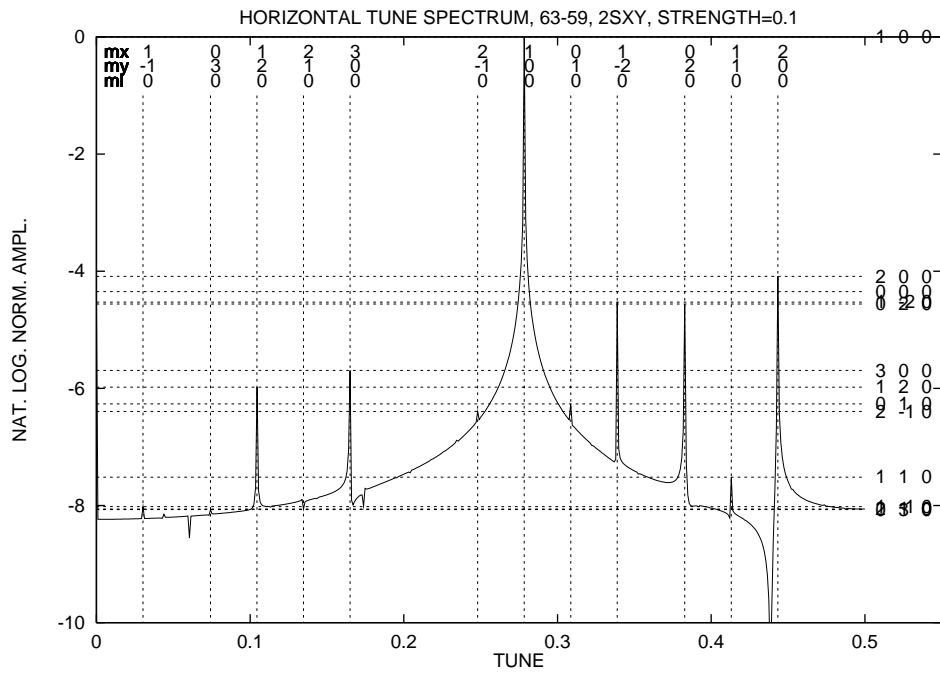


Figure 4.3: Spectral analysis of horizontal motion with systematic skew sextupole errors only and presently nominal tunes (63.28,59.31).

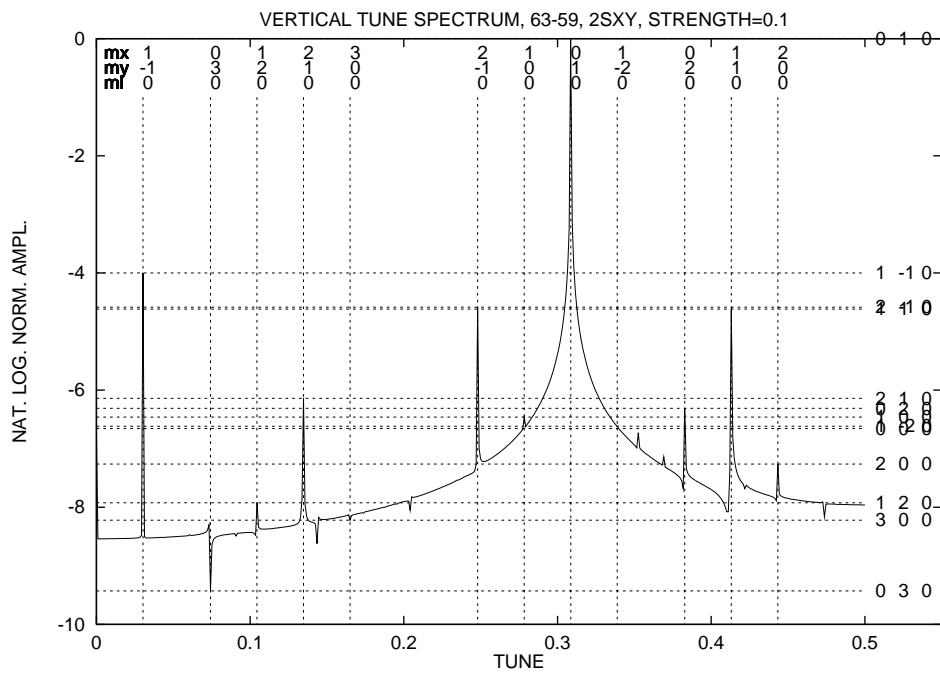


Figure 4.4: Spectral analysis of vertical motion with systematic skew sextupole errors only and presently nominal tunes (63.28,59.31).

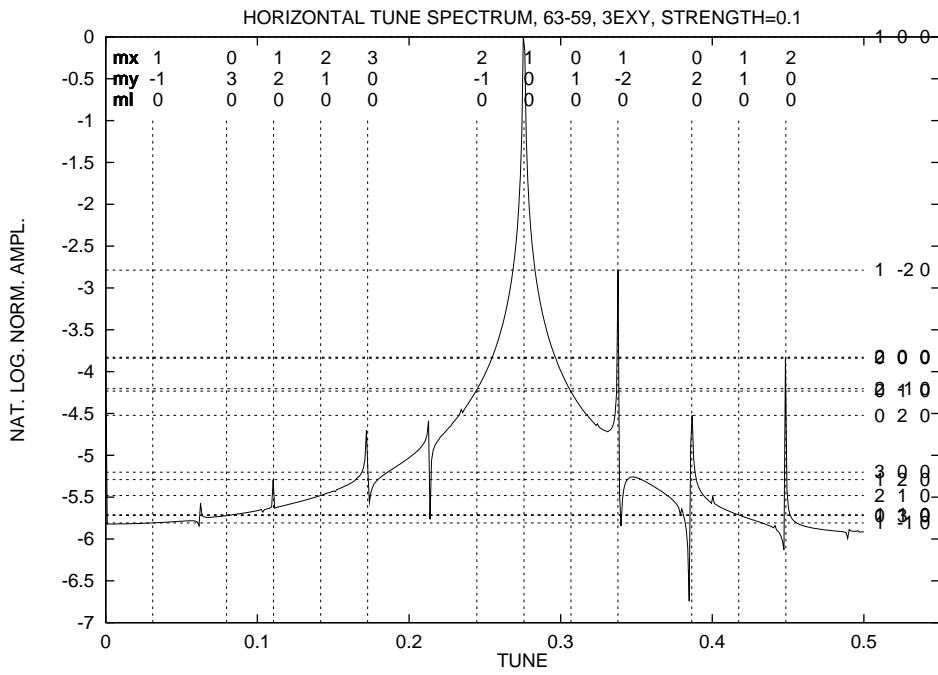


Figure 4.5: Spectral analysis of horizontal motion with systematic erect octupole errors only and presently nominal tunes (63.28,59.31).

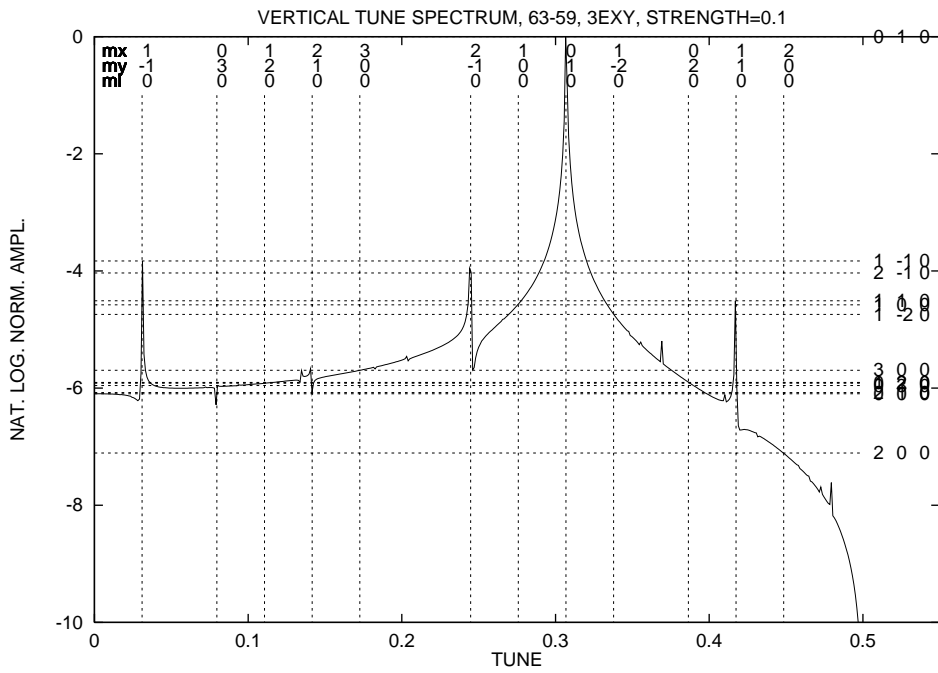


Figure 4.6: Spectral analysis of vertical motion with systematic erect octupole errors only and presently nominal tunes (63.28,59.31).

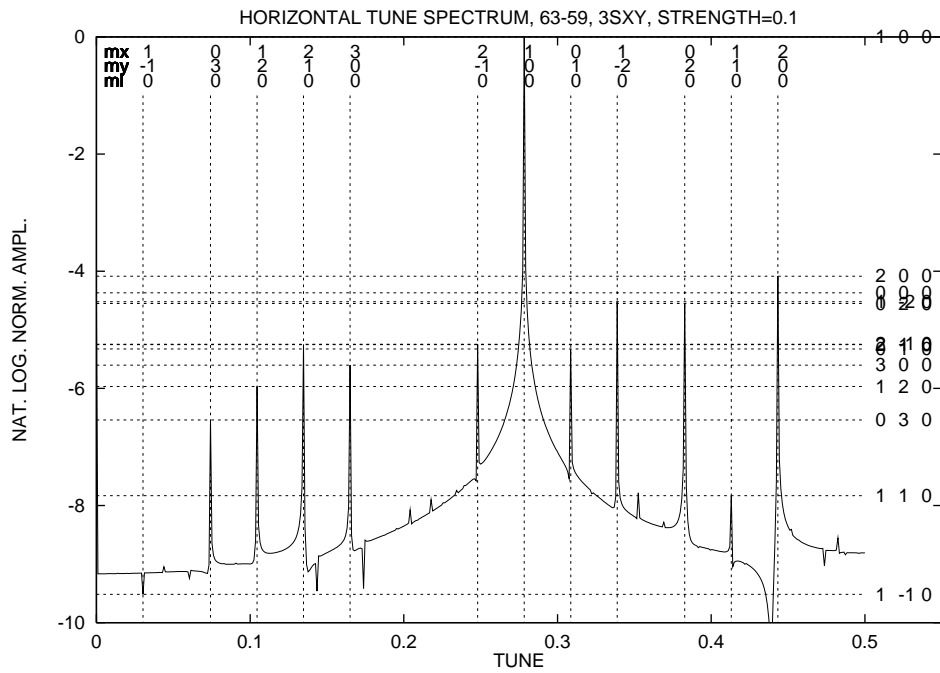


Figure 4.7: Spectral analysis of horizontal motion with systematic skew octupole errors only and presently nominal tunes (63.28,59.31).

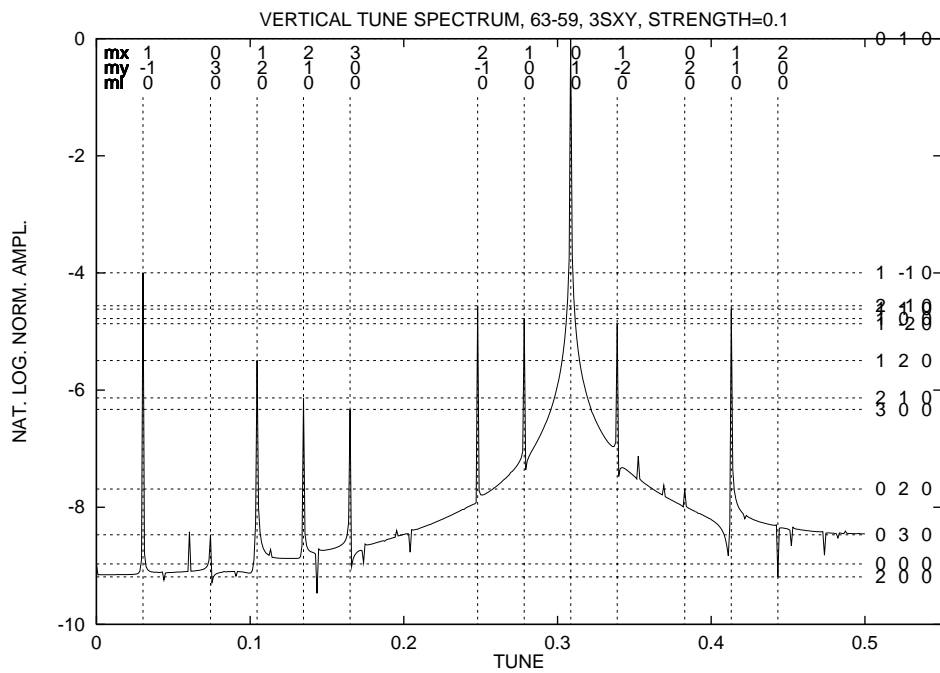


Figure 4.8: Spectral analysis of vertical motion with systematic skew octupole errors only and presently nominal tunes (63.28,59.31).

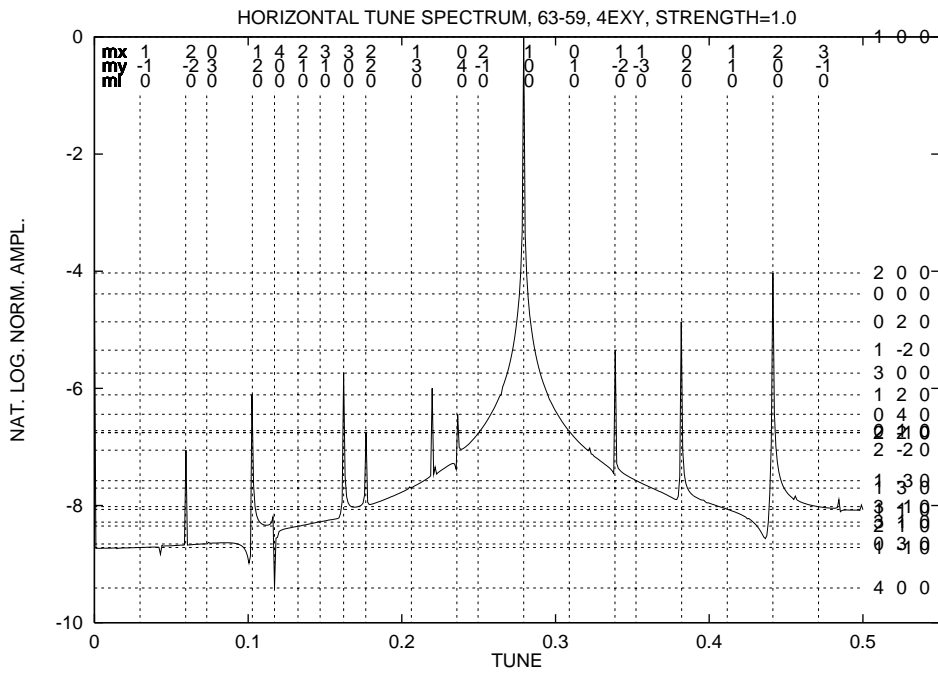


Figure 4.9: Spectral analysis of horizontal motion with systematic erect decapole errors only and presently nominal tunes (63.28,59.31).

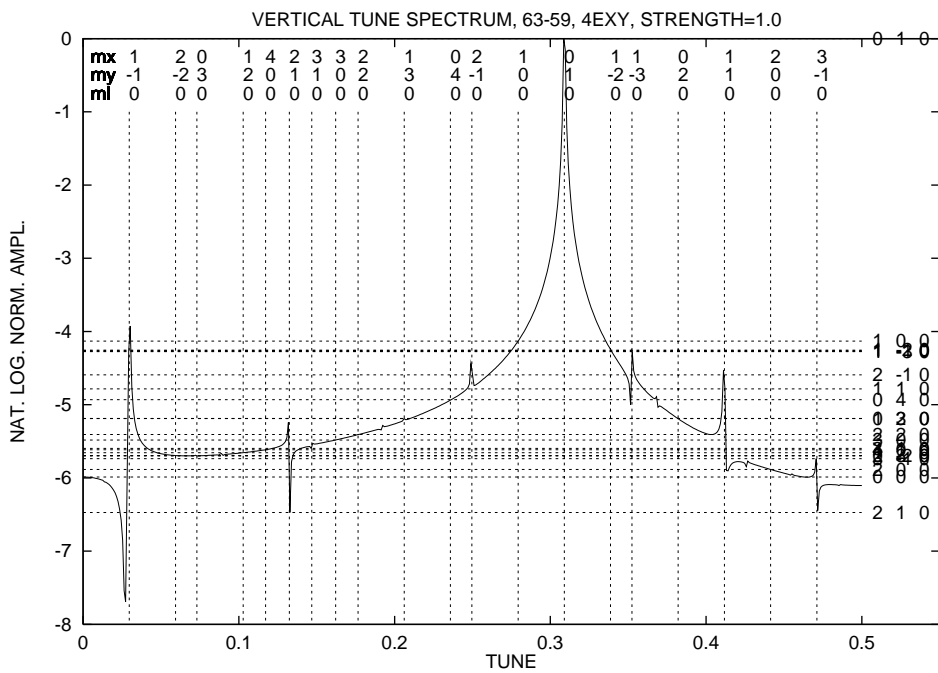


Figure 4.10: Spectral analysis of vertical motion with systematic erect decapole errors only and presently nominal tunes (63.28,59.31).

Table 4.1: Strengths of “clean” lines due to skew octupoles, as calculated and as extracted by FFT from element-by-element tracking.

horz/vert	m_x	m_y	predicted ratio	observed ratio
horz	2	1	0.0049	0.0057
	2	-1	0.0066	0.0062
	0	3	0.0014	0.0017
vert	3	0	0.0015	0.0021
	1	2	0.0040	0.0045
	1	-2	0.0073	0.0089

5. Conclusions

For the version of the LHC that has been investigated the optimal integer tunes have been shown to be $Q_x = 65$, $Q_y = 58$, and the previous paper showed that the dynamic acceptance for fractional tunes $Q_x = 0.28$, $Q_y = 0.31$ is optimal (almost anyway). Hence the tunes $Q_x = 65.28$, $Q_y = 58.31$ are unambiguously favored, at least for the LHC version studied in this report. It is my opinion that the same tunes are likely to remain favorable for more recent versions of the LHC but, of course, this should be checked.

It seems that the optimum is determined largely by two considerations, both of which will be somewhat different in the actual LHC from what has been assumed in this paper. The first of these considerations is cancellation per arc. The “trombones” used for adjusting the tunes in this study produce a different lattice than will the more polished retuning that will actually be used. (In particular the arc quad strengths will probably remain more nearly equal, since my phase trombones have been restricted to about 2/3 of each arc.) This difference may alter the superposition of nonlinear amplitudes over one arc appreciably. The optimum is also based on partial cancellation per whole lattice. This superposition is somewhat sensitive to details of straight section design and to the division of phase advance between arcs and straight sections.

Appendix A. Using LHC arcs as phase trombone*

The “qd” and “qf” main arc quads form two families that are the natural choice for small re-tunings of the lattice tunes Q_x and Q_y . For tune changes less than about 0.1 this re-tuning causes only moderate mismatching of the optics but, if one wishes to change the integer tune separation $Q_x - Q_y$ over the large range required for this study, unacceptably large β -waves develop unless the lattice is re-tuned. There are enough correction quadrupoles available to make this re-tuning straightforward, but it is desirable to have orthogonal “knobs” with the re-tuning already built in. Such knobs power a few normally-off trim quads with currents proportional to ΔQ_x when Q_x alone is being shifted or proportional to ΔQ_y (with different coefficients) when Q_y alone is being shifted.

ODD-EVEN ARCS		EVEN-ODD ARCS
qd/2	match point	qf/2
qtqf17, qf qtqd18, qd	trim section	qtqd17, qd qtqf18, qf
qtqf19, qf qtqd20, qd		qtqd19, qd qtqf20, qf
qf qd	6 full cells	qd qf
qf/2, qf/2		qd/2, qd/2
qd qf	6 full cells	qf qd
qtqd20, qd qtqf19, qf	trim section	qtqf20, qf qtqd19, qd
qtqd18, qd qtqf17, qf		qtqf18, qf qtqd17, qd
qd/2	match point	qf/2

Figure Appendix A.1: Long arc sections of the LHC that can function as “tune trombones”. Trombones on the left are contained in every second arc beginning with the one from IR1 to IR2. Their optical properties are trimmed using the four pairs of trim quads, qtqd17, qtqf18, qtqd19, qtqf20.

* This appendix is copied almost *verbatim* from LHC Project Note 130.²

A configuration that has proved to be capable of providing this functionality is shown in Fig. Appendix A.1. The sector between IR1 and IR2 (also 3-4, 5-6, and 7-8) is called “odd-even” and is shown on the left of the figure. The “even-odd” sectors differ by having horizontal and vertical elements interchanged as shown. In order to perturb the lattice minimally it is appropriate for the dominant families to have the largest possible number of elements situated in positions as nearly equivalent as possible. Toward that end, we have defined the arc regions between quad correctors “qtqf17..” as “phase trombones” and allowed the “qd” and “qf” elements in those regions to retain their names and to serve as the dominant tune shift families. Since these quads constitute about 2/3 of the quads of this class, their strengths per unit tune shift are about 3/2 as strong as if all “qd” and “qf” elements were used.

Gross tune changes desired are provided by all the 18 “qf” quads in one sector acting as one family and the 17 “qd” quads acting as another. It remains to tune out the β -waves engendered by these changes, and for that purpose we choose the 4 pairs of correction quads symmetrically placed and powered near the ends of the selected arc regions. Trim quadrupoles 17 through 20 are adjusted to maintain the Twiss function match at the centers of the “qd0” quadrupoles just outside the ends of the trombone section. (The strengths of these “qd0” quads and all other “qf0”’s and “qd0”’s outside the trombone are held fixed when the trombone is varied.) Since the sectors have been selected to be symmetric about the “qf” quad in the center, and since the nominal Twiss functions are similarly symmetric, the trim elements can also be symmetric as shown. For the first arc the pairs are “qt.qf17.r1, qt.qf17.l2” and “qt.qd18.r1, qt.qd18.l2” and “qt.qf19.r1, qt.qf19.l2” and “qt.qd20.r1, qt.qd20.l2”. The other arcs are similar.

All these tuning operations were performed using *TEAPOT*.

7. References

1. R. Talman, Tune Optimization for Maximum Dynamic Acceptance, I: Formulation, LHC Project Report 197, July, 1998.
2. N. Malitsky and R. Talman, Study of LHC Aperture Dependence on Tune Separation Using Thin Lenses, Phase Trombones, and “Unified Accelerator Libraries”, LHC Project Note 130, February, 1998.